Proceedings of the ASME 2011 Pressure Vessels & Piping Division Conference
PVP2011
July 17-21, 2011, Baltimore, Maryland, USA

PVP2011-57695

STUDY OF CREEP RELAXATION BEHAVIOUR OF 316H AUSTENITIC STEELS UNDER MECHANICALLY INDUCED RESIDUAL STRESS

Hamed Yazdani Nezhad*
Dept. of Mech. & Aero. Eng.,
Materials and Surface Science Inst.,
University of Limerick,
Limerick, Ireland

Noel P. O'Dowd
Dept. of Mech. & Aero. Eng.,
Materials and Surface Science Inst.,
University of Limerick,
Limerick, Ireland

Catrin M. Davies
Dept. of Mechanical Engineering,
Imperial College London,
South Kensington Campus,
London, SW7 2AZ, UK

Kamran M. Nikbin
Dept. of Mechanical Engineering,
Imperial College London,
South Kensington Campus,
London, SW7 2AZ, UK

Robert C. Wimpory
Helmholtz Zentrum Berlin,
Glienicker Strasse 100,
D-14109, Berlin,
Germany

ABSTRACT

Compact tension 316H austenitic steel specimens, extracted from an as-received ex-service pressure vessel header, have been pre-compressed to different load levels in order to introduce a residual stress field. Finite element (FE) analysis has been performed to predict the load level required to obtain a high magnitude tensile stress field over a significant distance ahead of the notch while preventing a large plastic zone in the specimen. The predicted residual stress profiles along the crack path are compared with those measured using neutron diffraction (ND). Comparisons have also been provided between the ND results of this work with recent work carried out on 316H and 347 stainless steels under different loading levels. The creep relaxation behaviour of the steel has been studied numerically. A proposed method to estimate the steady state creep crack tip parameter, C^*, has been examined using the obtained displacement rates for the case of combined loading. Creep relaxation data for combined stresses are compared with the earlier studies.

*Address all correspondence to this author.

1 INTRODUCTION

Studies of creep behaviour in critical structures such as nuclear power generation plants are important in the category of structural integrity assessment. Several procedures regarding structural integrity assessment have been standardised, e.g. R5 [2] and R6 [1], and can be used to evaluate the effect of defects and loading conditions on creep. The procedures cover topics such as creep behaviour under combined primary (mechanical) and secondary (thermal or residual) stresses [2].

Residual stress plays an important role in the study of creep relaxation (CR) and creep crack growth (CCG) in metallic components. The effects of tensile residual stress at the notch root of C(T) specimens (25mm thickness) subjected to pre-compression, extracted from a 316H steam header, on CR and CCG have been studied in [3] and [4] with no primary loads. In this work, the effect of incorporating primary loads on stress relaxation during creep are studied.

Numerical studies of CR at different residual stress level, under elastic conditions have been performed in [5] and have been extended to creep under elastic-plastic conditions in [6]. In the

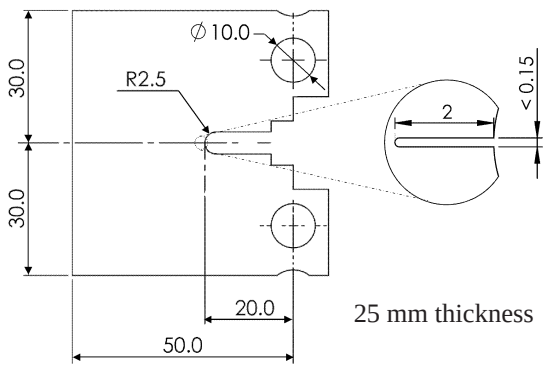

Figure 1. Schematic illustration of the C(T) specimen after EDM. All dimensions in mm.

earlier works [5, 6] simplified material models and residual stress distribution were examined. In this work, the residual stress (RS) distributions are obtained from pre-compressed C(T) specimens and a more representative elastic-plastic creep material model is used. In order to quantify the RS magnitude and relaxation, ND measurements were performed on the pre-compressed 316H C(T) specimens.

2 SPECIMEN GEOMETRY AND MATERIAL

Four C(T) specimens, all having 25 mm thickness and 50 mm width, were extracted from an as-received ex-service header manufactured from 316H austenitic steel. The specimens were subjected to pre-compression and then pre-cracked using electro-discharge machining (EDM). Figure 1 shows the specimen dimensions (Note that the loading pin holes are inserted after pre-compression.). Tensile test specimens were also extracted from the header and were subjected to uniaxial tension at room temperature to obtain the stress-strain behaviour (Fig. 2). A number of tests at different strain rates have been performed to ensure the material rate independence. Comparison with the recent data from a different 316H-header [4] (triangle symbols in Fig. 2) shows nearly the same Young's modulus and hardening behaviour though the current test (square symbols in Fig. 2) shows approximately a 40 MPa lower yield stress. Tensile test data at 550° have been provided for this material in [7] and are also used in this work.

3 BACKGROUND

Creep relaxation behaviour under combined mechanical and residual stresses have been studied for single edge notch bend, SEN(B), and tension, SEN(T), specimens for shallow cracks ($a/W = 0.07$ and 0.15 with a the crack length and W the specimen width) under elastic [5] and elastic-plastic [6] conditions.

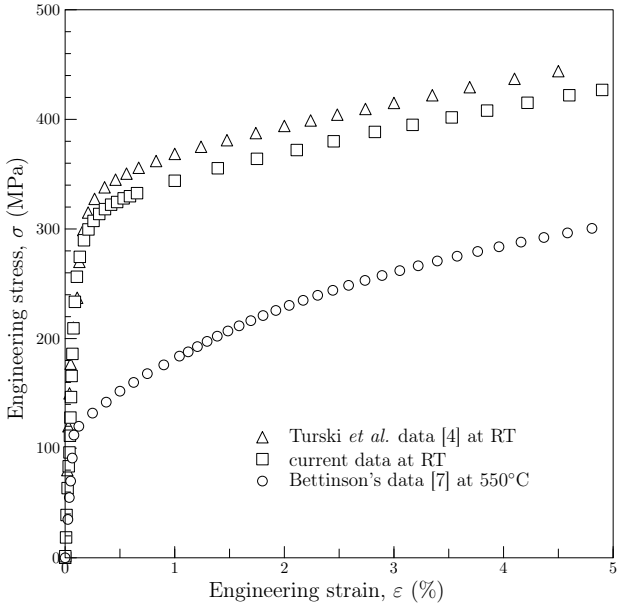

Figure 2. Tensile data for the 316H austenitic steel at room temperature (RT) and 550°C

This work extends those studies to C(T) specimens with deeper cracks size ($a/W \geq 0.44$). The transient creep crack tip parameter, $C(t)$, used to identify the stress and strain distribution (see e.g. [8]), is defined by

$$C(t) = \int_{\Gamma \to 0} \dot{W}(\dot{\varepsilon}) dy - \mathbf{t} \frac{\partial \dot{\mathbf{u}}}{\partial x} ds, \tag{1}$$

where

$$\dot{W}(\dot{\varepsilon}) = \int \boldsymbol{\sigma} d\dot{\varepsilon} \tag{2}$$

is the strain energy rate density and $\dot{\varepsilon}$ is the creep strain rate. The creep strain rate can often be related to the stress σ, by a power law relation

$$\dot{\varepsilon} = A\sigma^n, \tag{3}$$

where A and n are material constants. $C(t)$ is evaluated over paths very close to the crack tip ($\Gamma \to 0$). During the steady state creep regime, under constant stress, the value of $C(t)$ becomes both time and path independent, denoted by C^*. The value of C^* is independent of secondary stress, as self-equilibrating stress distributions will relax over long times.

For a power law creeping material, C^* may be estimated experimentally from the load and load line displacement (LLD) or

(crack) mouth opening displacement (MOD) rate measurements using the relations [9]

$$C^*_{LLD} = \frac{P\dot{\Delta}_{LLD}}{B(W-a)}\frac{N}{N+1}\eta_{LLD}, \tag{4}$$

$$C^*_{MOD} = \frac{P\dot{\Delta}_{MOD}}{B(W-a)}\frac{N}{N+1}\eta_{MOD}, \tag{5}$$

respectively, with P the load, B the net thickness, N the hardening exponent and geometry dependent factor of η [9]. Both C^*_{LLD} and C^*_{MOD} values have been obtained from the FE analysis. Here $\dot{\Delta}_{LLD}$ is obtained from load point displacement and $\dot{\Delta}_{MOD}$ is obtained from crack mouth opening displacement (see Figs. 3 and 4). The values for displacement rate ($\dot{\Delta}$) are obtained in the secondary (steady state) regime.

The data used for the creep behaviour in the secondary regime have been taken from the earlier work on 316H [10]. For the secondary creep response

$$\begin{cases} A = 1.47\times10^{-34} \\ n = 11.6 \end{cases} \tag{6}$$

in eq. (3) (stress in MPa, time in hr.) was found to fit the data in [10].

A redistribution time, t_{red}, may be defined, which represents the time for $C(t)$ to reach its steady state value of C^* [11]. This value may be approximated by the relation,

$$t_{red} = \frac{J_0}{C^*}. \tag{7}$$

Here J_0 is the initial J value, which in this work, includes the contribution of residual stress. Under small scale yielding conditions,

$$J_0 = \frac{(K^p + K^s)^2}{E'}, \tag{8}$$

where K^p and K^s are (initial) primary and secondary stress intensity factors prior to creep, respectively, and E' is the effective Young's modulus, where $E' = E/(1-\nu^2)$.

Creep relaxation behaviour for a power law material can be estimated using t_{red} (see e.g. [8]) by

$$\frac{C(t)}{C^*} = \frac{(1+t/t_{red})^{n+1}}{(1+t/t_{red})^{n+1} - \phi}, \tag{9}$$

where, as proposed in [12]

$$\phi = 1 - \frac{C_N C^*}{AJ_0}. \tag{10}$$

C_N depends on the elastic-plastic response of the material and is given as

$$C_N = \frac{1}{E'\sigma_y^{N-1}}, \tag{11}$$

with σ_y the yield stress. The parameter ϕ depends on the degree of initial plasticity taking the value of unity for elastic-creep behaviour and zero under widespread plasticity. Note that eqs. (9) and (10) were derived for load control conditions and $n = N$ [12]. The majority of elastic-plastic creep studies to date have used the latter assumption. Results will be presented in section 7.

4 FINITE-ELEMENT MODEL

Two and three dimensional (2D and 3D) FE analyses have been carried out. The 3D model is shown in Fig. 3. Refined elements have been constructed around the notch root to allow an accurate extraction of the notch tip parameters. Two dimensional 4-node quadratic elements have been used to discretise the model. Linear 'hybrid' plane strain and plane stress elements (CPE4H and CPS4 in ABAQUS [13]) have been used and 8-node hexahedron elements (C3D8) have been used in the 3D analysis. Both isotropic hardening and linear kinematic hardening behaviour have been used to model the plastic behaviour of the material. Linear kinematic hardening stress and strain data have been extracted by taking a linear regression from the tensile test data presented in Fig. 2.

5 PRE-COMPRESSION TESTING AND CONDITIONS

Compact tension specimens have been pre-compressed with loads (P in Fig. 4) of 53 kN (labeled as A1B1 and A1B2) and 65 kN (labeled as A1B4) to induce tensile residual stress fields ahead of the notch after unloading.

Two criteria were applied to determine the loading level: obtaining the highest possible tensile stress values ahead of the notch and avoiding large plastic deformation in the specimen ($\varepsilon^{pl}_{eq} < 0.1\%$ with ε^{pl}_{eq} the equivalent plastic strain). Figure 5 shows the equivalent strain contours from a typical FE analysis. The shaded region corresponds to the high plastic strain region as $\varepsilon^{pl}_{eq} \geq 0.1\%$. As seen in Fig. 5, loading levels must be carefully controlled to avoid excessive plastic deformation that may lead to cracking prior to creep deformation. Based on these studies, 53 and 65 kN have been chosen to represent low and high secondary stress levels, respectively, in C(T) specimens.

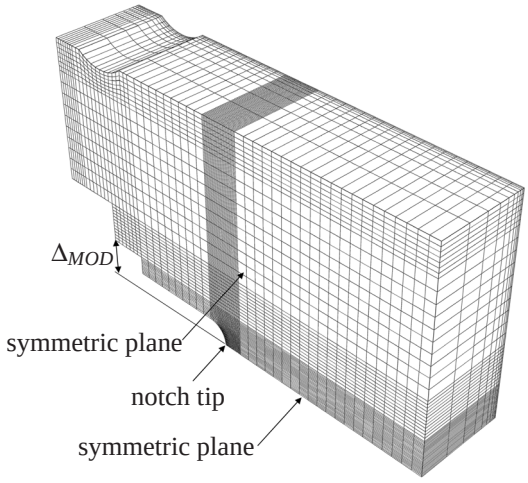

Figure 3. Typical three dimensional FE model

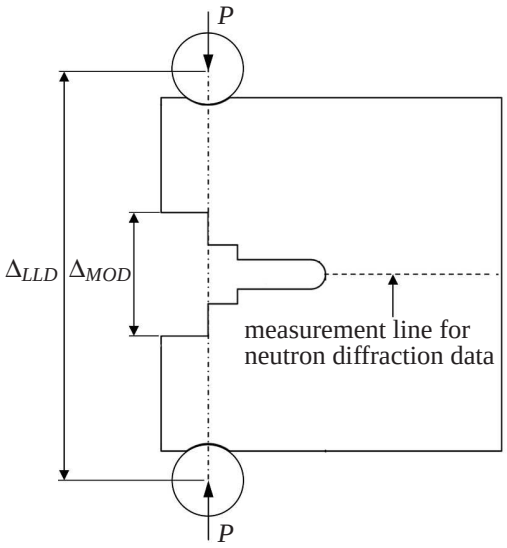

Figure 4. Schematic of the C(T) specimen under compression

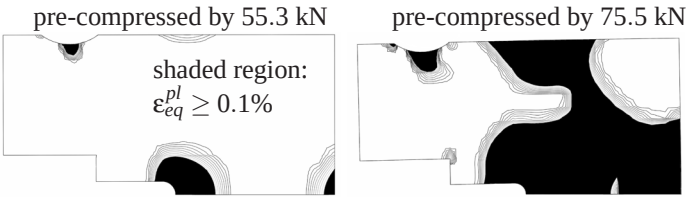

Figure 5. Evolution of contours of ε_{eq}^{pl} in the C(T) specimen at different loading level

6 RESIDUAL STRESS REDISTRIBUTION

Non-destructive neutron diffraction is required to penetrate sub surface to a sufficient depth to quantify the residual stresses ahead of the notch (see Fig. 4). ND measurements have been carried out at E3, Helmholtz-Zentrum Berlin (HZB). A gauge volume of $3\times3\times3$ mm^3 for A1B1 and A1B4 and $4\times4\times4$ mm^3 for A1B2 was used. For each specimen, measurements were taken at 20 to 30 points ahead of the notch along the crack path with a measuring time of approximately 30 minutes per point.

6.1 Comparisons between residual stress redistributions measured using ND in 316H and 347 C(T) specimens

Residual stress profiles in 316H and 347 C(T) specimens were compared in [14] with pre-loads of 110 kN for 316H and 150 kN for 347 stainless steel C(T) specimens. Results were taken from [15] for 347 and from [4] for 316H. This work extends comparisons carried out in [14] to different loading levels. Figure 6 compares the normalised residual stress ($\sigma_{22}/\sigma_{0.2}$ with $\sigma_{0.2}$ the 0.2% proof stress) obtained from the ND measurements. As seen, the normalised results are almost independent of the steel type and loading level. Results also show that plastically induced residual stresses produce near yield stress levels under 65 kN pre-compression and hence further compression (110 kN) does not significantly affect this level. However, it should be noted that stress levels may be higher near the notch which are not well resolved by the ND technique due to surface effects. High energy X-ray diffraction (HEXRD) measurements [4] have shown high strain values close to the notch tip. Thus the ND measurement in Fig. 6 may not be resolving the stress near the notch root due to the high gauge volume factor.

6.2 Comparisons between residual stress redistributions from ND measurements and the FE analysis

A comparison between measured and predicted RS profiles is provided in Fig. 7. In Fig. 7(a), comparisons are provided between the ND data and FE results for a C(T) specimen with the 53 kN pre-compression load. The FE analyses have been carried out using both isotropic and linear kinematic hardening assumptions. As seen in Fig. 7(a), the stress predicted from the 3D FE analysis is high near the notch and, though not shown here, in close agreement with the results from a 2D plane strain FE analysis. The plane stress FE analysis predicts lower stress values near the notch. It is also seen that good agreement has been obtained between the ND data and results from the plane stress analysis. The result that the plane stress FE prediction appears to provide better agreement with the measured stress than the 3D prediction is unexpected and may be fortuitous. This result is under investigation. Results from the FE analysis with linear kinematic hardening assumption predict lower stress values, providing a better agreement with the ND data compared to

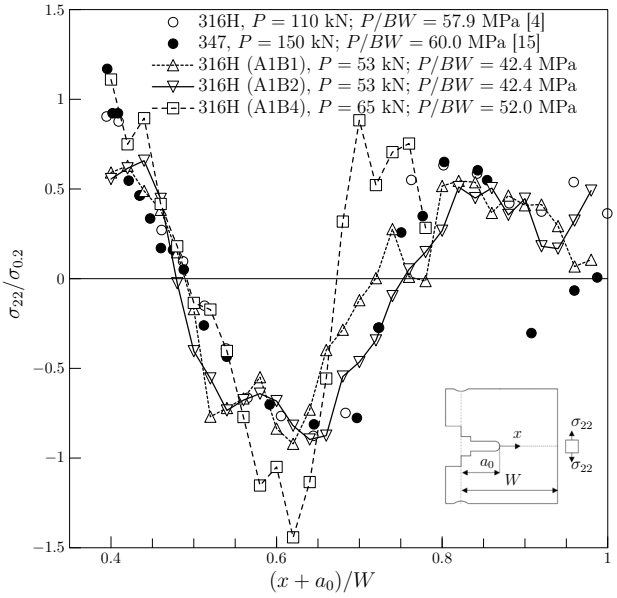

Figure 6. Measured residual stress distributions for 316H and 347 C(T) specimens after pre-compression, normalised by 0.2% proof stress ($\sigma_{0.2}$)

the results from the isotropic hardening analysis. Similar conclusions were reported in [4] for 316H and in [15] for 347 stainless steel material. The results from isotropic and kinematic hardening models are in good agreement far away from the notch root, $x > 2.5$ mm.

For the 65 kN load case reasonable agreement between the ND measurements and plane stress FE analysis is also seen in Fig. 7(b). Note, however, that in this case the stress at the notch root is best predicted by the 3D kinematic hardening analysis. The 3D FE analysis predicts a 3 mm tensile stress region, approximately, ahead of the notch, 4 mm for plane stress analysis and 2.5 mm for plane strain analysis. To ensure that the crack lying in the tensile region, a 2 mm slot has been machined using EDM (Fig. 1).

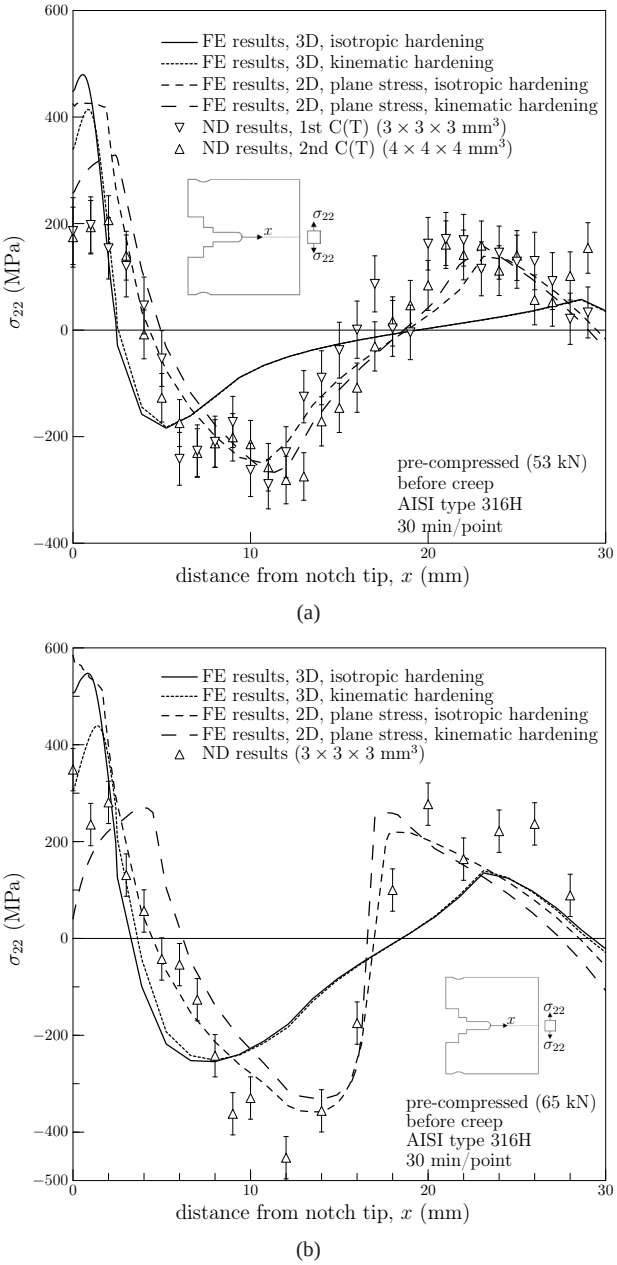

Figure 7. Measured stress versus distance from tip; (a) pre-compressed C(T)s by 53 kN, (b) pre-compressed C(T) by 65 kN, before creep, 25mm thickness

7 CREEP RELAXATION IN 316H C(T) SPECIMEN

7.1 Prediction of stress redistribution

Stress relaxation occurs during creep and in the steady state creep regime, the steady state creep crack tip parameter, C^*, can be obtained either directly from the FE analysis based on eq. (1) or from the approximations based on eqs. (4) and (5). It has been found in this work that C^*_{MOD} values are in close agreement with the FE values of C^* at long times.

The pre-compression discussed in section 5 is carried out at room temperature. A crack is introduced ahead of the notch. The specimen is then heated to 550°C and the creep load is applied. During the heating-up process, the material behaviour is allowed to change from its values at room temperature to those at 550°C (Fig. 2). The value of $C(t)$ is taken to be the average of values over five element rings around the crack tip node (first ring excluded) from the FE analysis. Our investigations show that the maximum difference in $C(t)$ values over these contours, when

$t/t_{red} = 0.001$, is approximately 8% for $K_i^p = 25$ MPa$\sqrt{m}$ (the worst case). Results from [3] showed that a major proportion of creep damage within the specimen, due to the thermal soaking, occurs during the first 1000 hours. Thus this time duration has been taken for the creep tests and simulations in this work.

Figure 8 shows the predicted stress redistribution ahead of the notch of the specimens pre-compressed by the load of 53 kN. As seen in Fig. 7, the plane stress analysis provides a better agreement with the ND data and therefore a plane stress analysis was used to investigate the stress relaxation. The mechanical load (identified by K_i^p) examined in the FE analysis, has been selected to be in the range of 20 to 25 MPa$\sqrt{m}$. For the C(T) specimen, K_i^p is defined by the relation (see e.g. [1])

$$K_i^p = \frac{P}{BW^{1/2}} \left(\frac{2+a/W}{1-a/W^{3/2}} \right) f(a/W), \tag{12}$$

where P is the mechanical load during creep and the non-dimensional function of $f(a/W)$ is obtained by

$$\begin{aligned} f(a/W) = 0.886 + 4.64(a/W) - 13.32(a/W)^2 \\ +14.72(a/W)^3 - 5.60(a/W)^4. \end{aligned} \tag{13}$$

Figure 8(a) shows the predicted stress redistribution results from the FE analysis. The solid line presents the results after introducing the crack in the model loading to a peak stress of 480 MPa. The results show that the maximum normal stress at the crack tip relaxes to about 50% of its initial value after one hour at temperature 550°C. A mechanical load is then applied which increases the stress close to the room temperature value. Figure 8(a) shows that an approximate 140 MPa drop in stress values is seen after creep for 1000 hrs. at 550°C.

In Fig. 8(b) the plane strain results are presented. As seen, the plane strain analysis predicts a high peak stress after crack introduction and a high stress gradient near the crack tip. Slight relaxation due to creep is seen for plane strain conditions (approximately 30 MPa drop near the crack tip) compared to the plane stress results in Fig. 8(a) with 140 MPa drop in stress values over 1000 hours.

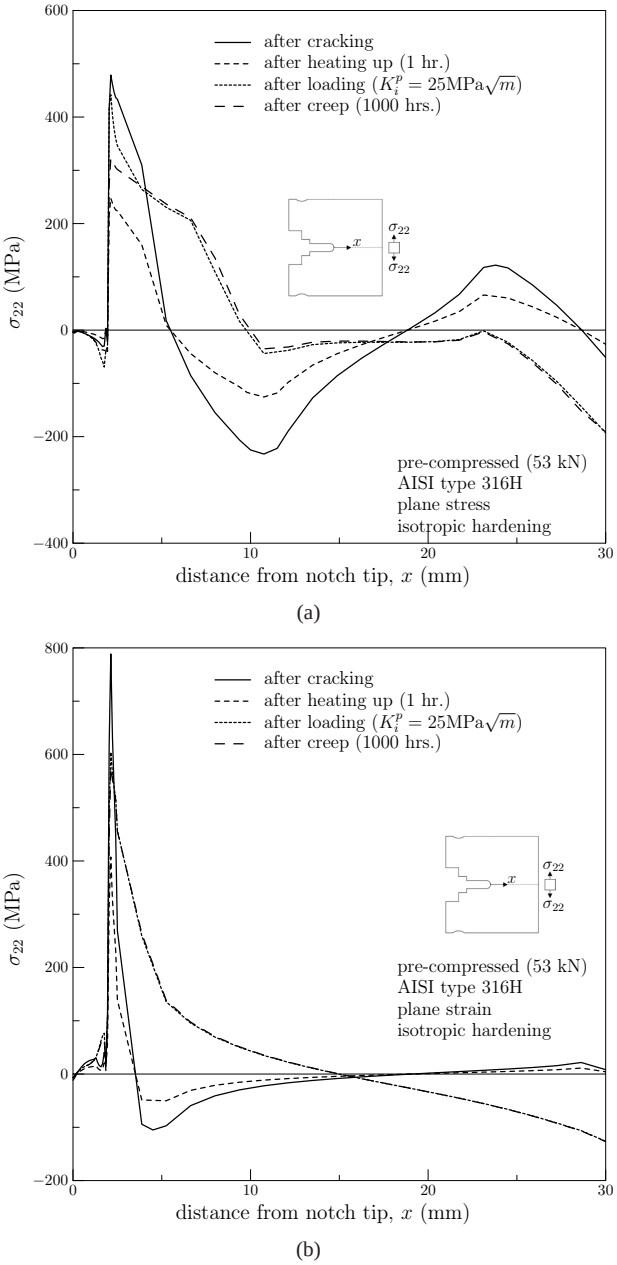

Figure 8. Normal stress distributions from the FE analysis for 316H C(T) specimens pre-compressed by 53 kN ($K^s = 25.9$) under $K_i^p = 25$ MPa$\sqrt{m}$; (a) plane stress, (b) plane strain

7.2 Crack tip parameter under combined residual and mechanical stresses

Residual J values have been obtained after introducing the crack ($a/W = 0.44$) using the modified J expression in [16], which provides a path independent J-integral. The value of the secondary stress intensity factor (K^s) has been obtained from the J-integral, $K^s = \sqrt{JE'}$, as 25.9 and 33.4 MPa$\sqrt{m}$ for 53 and 65 kN respectively. The values of K^s are used in eq. (8) to calculate the initial J, designated J_0, from eq. (8) and also provide an estimate of t_{red} from eq. (7). The relation between K_i^p and C^* has been obtained numerically and is shown in Fig. 9. Note that C^* is not sensitive to K^s. The values of C^* obtained from eqs. (4) and (5) are also included in this figure. For this value of a/W, $\eta_{LLD} = \eta_{MOD} = 2.2$ [17] - the difference between the two estimations arises from different values of $\dot{\Delta}_{MOD}$ and $\dot{\Delta}_{LLD}$.

The FE results for the $C(t)$ parameter are shown in Fig. 10

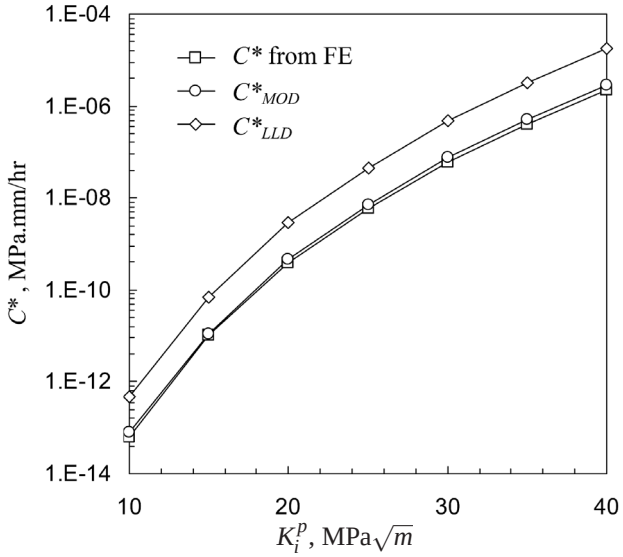

Figure 9. C^* versus K_i^p from the FE analysis for 53 kN pre-compressed 316H C(T) specimen ($K^s = 25.9$ MPa$\sqrt{m}$)

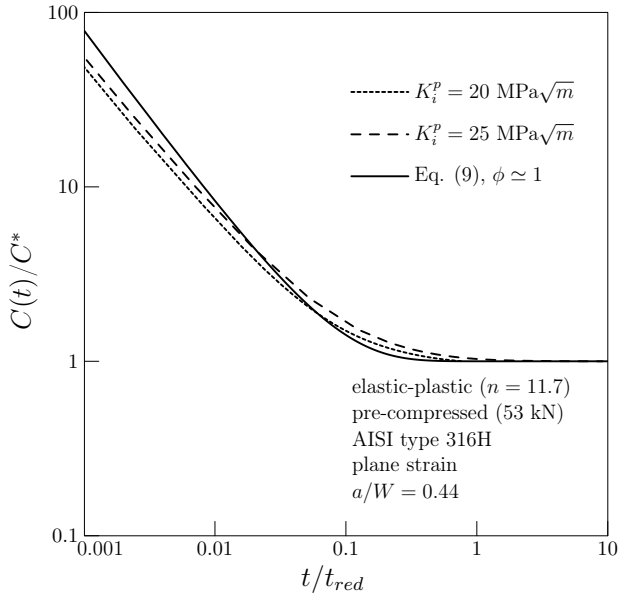

Figure 10. Comparison of evolution of $C(t)$ in 53 kN pre-compressed C(T) specimen at different primary loads (K_i^p)

for C(T) specimens pre-compressed by the load of 53 kN ($K^s = 25.9$ MPa$\sqrt{m}$) and subjected to primary load, K_i^p (20 MPa$\sqrt{m}$ and 25 MPa$\sqrt{m}$), during creep. The redistribution time, t_{red}, has been obtained from eq. (7) based on the FE values of C^* and J_0. The analytical $C(t)$ results (presented by a solid line) obtained from eq. (9), are in close agreement with the FE results. As also seen, the time for $C(t)$ to reach its steady state value is closely predicted by eq. (7), i.e. $C(t) \to C^*$ as $t \to t_{red}$ (as found in [5] and [6] for different geometries and $n = 10$).

8 CONCLUSIONS

Residual stress generation and creep relaxation behaviour of pre-compressed compact tension 316H specimens have been studied in this work. Finite element analyses were performed to predict the load level required to obtain a high magnitude tensile stress field. The residual stress field was measured using the ND technique and compared to FE results, showing good agreement. It was found that the normalised RS profile obtained for 316H and 347 stainless steel is weakly dependent on the pre-compression level and the specimen size. Creep relaxation behaviour was also studied numerically and it was found that C^* can be closely represented by C^*_{MOD} rather than C^*_{LLD}.

The values of $C(t)/C^*$ for the case of combined stresses in C(T) specimens pre-compressed by the load of 53 kN, were obtained numerically and analytically. The results show that eq. (9) provides good agreement with the FE results. It was also found that stress relaxation under combined primary and secondary stress can be characterised using the redistribution time, t_{red} and eq. (9), i.e. $C(t)$ approaches C^* as t approaches t_{red}, in agreement with the earlier studies in [5] and [6]. These results will provide preliminary data for the creep crack growth tests currently under development.

ACKNOWLEDGMENTS

Financial support for this work has been provided by Science Foundation Ireland under grant 08/RFP/ENM1477. Helpful discussions on numerical methods with Dr Dongfeng Li at the University of Limerick, Dr Simon Kamel and Ali N. Mehmanparast from Imperial College London are gratefully acknowledged. Computational work was carried out using the MSSI AMPS cluster, enabled under the framework of the INSPIRE programme, funded by the Irish Government's Programme for Research in Third Level Institutions, Cycle 4, National Development Plan 2007-2013. ND measurements have been supported by the European Commission under the 7th Framework Programme through "Research Infrastructures" action of the "Capacities" Programme, contract number CP-CSA_INFRA-2008-1.1.1. Number 226507-NMI3.

REFERENCES

[1] R6, Revision 4, 2009, "Assessment of the Integrity of Structures Containing Defects", British Energy Generation Ltd., Gloucester, UK.

[2] R5, Revision 3, 2003, "An Assessment Procedure for the

High Temperature Response of Structures", British Energy Generation Ltd., Gloucester, UK.

[3] Turski, M. (2004) High Temperature Creep Cavitation Cracking under the Action of Residual Stress in 316H Stainless Steel, unpublished thesis (Ph.D.), Manchester Materials Science Centre, University of Manchester.

[4] Turski, M., Bouchard, P.J., Steuwer, A., Withers P.J., 2008, "Residual Stress Driven Creep Cracking in AISI Type 316 Stainless Steel", *J. Acta Materialia*, **56**(14), pp. 3598—3612.

[5] Yazdani Nezhad, H., O'Dowd, N.P., 2010, "Prediction of Transient Creep Response under Combined Primary and Secondary Loading", *Proceedings of the ASME 2010 Pressure Vessels & Piping Division/K-PVP Conference.*, Bellevue, WA, USA, 18-22 Jul.

[6] Yazdani Nezhad, H., O'Dowd, N.P., "Study of Creep Relaxation under Combined Mechanical and Residual Stresses", submitted for publication.

[7] Bettinson, A.D. (2002) The Influence of Constraint on the Creep Crack Growth of 316H Stainless Steel, unpublished thesis (Ph.D.), Department of Mechanical Engineering, Imperial College London.

[8] Webster, G.A., Ainsworth, R.A., 1994, "High Temperature Component Life Assessment", Chapman & Hall, London, UK.

[9] Davies, C.M., Mueller, F., Nikbin, K.M., O'Dowd, N.P., Webster, G.A., 2006, "Analysis of Creep Crack Initiation and Growth in Different Geometries for 316H and Carbon Manganese Steels", *J. ASTM international*, **3**(2).

[10] Davies, C.M. (2006) Crack Initiation and Growth at Elevated Temperatures in Engineering Steels, unpublished thesis (Ph.D.), Department of Mechanical Engineering, Imperial College London.

[11] Ainsworth, R.A., Budden, P.J., 1990, "Crack Tip Fields under Non-steady Creep Conditions -1. Estimates of the Amplitude of the Fields", *Fatigue Fract. Eng. Mater. Struct.*, **13**(3), pp. 263–276.

[12] Joch, J., Ainsworth, R.A., 1992, "The Effect of Geometry on the Development of Creep Singular Fields for Defects under Step-load Controlled Loading", *Fatigue Fract. Eng. Mater. Struct.*, **15**(3), pp. 229–240.

[13] ABAQUS v6.9. User's Manual. Inc. and Dassault Systems.

[14] Turski, M., Wimpory, R.C., O'Dowd, N.P., Withers, P.J., Nikbin, K.M., 2007, "A Comparison of Measurement and Modelling of Plastically Induced Residual Stresses in a 316H and a Weld 347 Stainless Steel", *Proceeding of Eight International Conference on Creep and Fatigue at Elevated Temperatures (CREEP8).*, San Antonio, Texas, USA, 22-26 Jul.

[15] O'Dowd, N.P., Nikbin, K.M., Wimpory, R.C., Biglary, F.R., O'Donnell, M.P., 2008, "Computational and Experimental Studies of High Temperature Crack Initiation in the Presence of Residual Stress", *J. Press. Vessel. Technol.-Trans. ASME*, **130**(4), 041403.

[16] Lei, Y., 2005, "*J*-integral Evaluation for Cases Involving Non-proportional Stressing", *Eng. Fract. Mech.*, **72**(4), pp. 577–596.

[17] Davies, C. M., Kourmpetis, M., O'Dowd, N. P., Nikbin, K. M., 2006, "Experimental Evaluation of the J or C^* Parameter for a Range of Cracked Geometries", *J. ASTM International*, **3**(4).